Thermochimica Acta, 39 (1980) 81—93

BROAD RANGE PURITY ANALYSIS BY MELTING POINT DEPRESSION USING A SINGULAR FEATURE COMMON TO ALL DSC PURITY SCANS

GRANT M. GUSTIN

Chemical Research Division, Norwich-Eaton Pharmaceuticals, Division of Morton-Norwich Products, Inc., Norwich, NY (U.S.A.)

(Received 5 March 1979)

ABSTRACT

DSC purity assay by melting point depression has had a limited range of less than several percent impurities. Step-mode heating techniques have increased the range to 6—8%. However, empirical corrections were used to linearize the purity slope of the van't Hoff plot, temperature vs. reciprocal of fraction melted ($1/F$).

A unique feature common to all dynamic purity scans has been discovered which matches a point on the non-linear van't Hoff plot to the heating rate. This point, or reciprocal of the melt fraction ($1/F$), occurs where the melting rate has attained maximum acceleration. The melting rate at this point is used as a tangential straight line projection from the curve to become a function of mole % impurity. The melting rate at maximum acceleration is independent of reference material, heating rate, sample size, thermal conductivity, or specific heat.

Phenacetin, spiked with 50 mole % benzamide, has been measured to ±2 mole % at heating rates of 5 and 10°C min^{-1}; the restriction on upper detection limits is adequate resolution between preliminary eutectic events and the final melt. Impurities in indium, with a reported purity of 99.9999%, have been measured at 4×10^{-5} mole % by this technique.

INTRODUCTION

Determining impurities by measuring the lowered melting point of a compound has a special appeal as a non-destructive and independent method of analysis. Two distinct techniques have evolved using differential scanning calorimetry: dynamic and step-mode scanning. The first, dynamic scanning [1,2], was limited to several percent of impurities. Exhaustive studies of the procedure [3,4] gave no significant improvements, leading to the conclusion that the van't Hoff law from which the computations were made was not valid beyond the 2% level [3]; yet this technique was of sufficient importance and utility that the United States Pharmacopeia devoted a section to it as an assay procedure [5]. Increasing the useful range to 6—10% occurred with step-wise heating [6]. This reportedly circumvented some baseline problems noted in the dynamic scan procedure, namely specific heat and thermal resistance [2]. Subsequent studies of this technique [7,8] and automation of the stepping procedure [9] have been reported.

Theoretically the van't Hoff expression

$$T_s = T_0 + \frac{XRT_0^2}{H}\frac{1}{F} \quad (1)$$

gives a straight line plot of temperature (T_s) vs. reciprocal of the fraction melted ($1/F$). T_0 represents the theoretical melting point of the pure substance, H is the molar heat of fusion, R is the gas constant (1.987 cal mole^{-1} T^{-1}), and X is the mole fraction of impurities in the resulting slope, $(XRT_0^2)/H$. However, failure to attain this straight line in practice has led to empirical correction techniques [2,3,4,9] for obtaining the best fit of a straight line to the van't Hoff curve. As higher levels of impurities increased the curvature, the applicability of the corrections deteriorated.

The van't Hoff plot of a typical dynamic DSC scan results in a curve shown in Fig. 4. The temperature scale is the programmed temperature reading at each data point, not altered with corrections recommended in ref. 1 which used the melting slope of a reference standard such as indium. This curve is affected considerably by heating rate, sample size, and thermal conductivity.

Since gross estimates of impurities have been visually discernable in dynamic curve traces [1], a certain unique feature of the curve would seem to be consistent with the impurities present in a more exact manner. In search of this feature, a study of the various curve characteristics was pursued.

NEW DYNAMIC PURITY METHOD

One feature of the melting process has been found to be unaffected by the variables mentioned above. At the point of maximum melting acceleration, the relationship between the melt fraction ($1/F$), melting rate, and heating rate becomes a function of the impurity level. This feature provides a tangential straight line projection from the curve in Fig. 4 to the theoretical (pure sample) melting point, T_0, where $1/F = 0$. Impurities ranging from 1 to 51% in Table 1 gave results by this technique within ±5% (RSD).

Equipment

A Perkin-Elmer model DSC-2 differential scanning calorimeter was used for the melt scans. All materials were sealed in volatile sample pans to avoid volatilization losses. The scan signals were recorded by an Infotronics model CRS-30 printing integrator with selectable integration periods as noted below.

The usual dynamic scan procedure is used to generate a typical endothermic melt curve shown in Fig. 1. The eutectic, or pre-melt region, is also measured as an essential part of the total heat of fusion. Failure to include it in the past contributed to the arbitrary corrections of the melt baseline and heat of fusion [1,3,4]. Inclusion of this region showed no corrections were needed [6]. The curve signal is integrated at fixed time periods; 1 or 2 sec

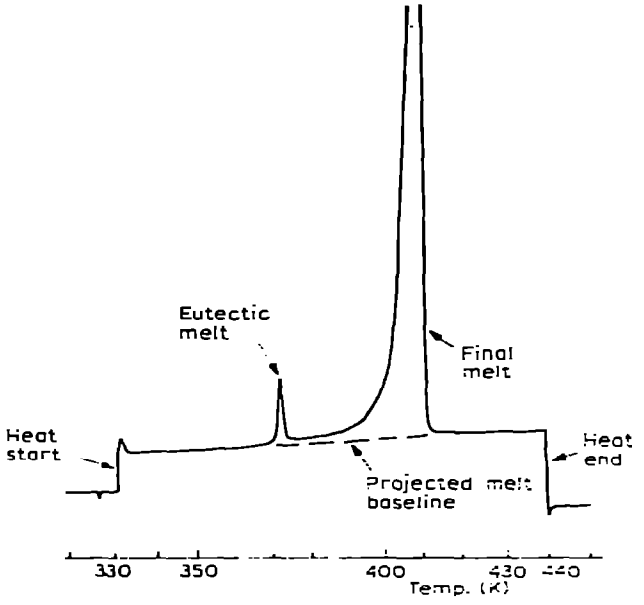

Fig. 1. Typical DSC scan for phenacetin with 3.03 mole % benzamide. Chart speed 0.5 in. min^{-1}; range 4 mcal sec^{-1}; sample weight 3.272 mg; molecular weight 197.2; initial temperature 330 K; final temperature 440 K; heating rate 10°C min^{-1}.

periods for extremely pure materials such as indium, and 4—12 s periods for melts having a broad temperature base such as in Fig. 1. Integration is started before the melt or eutectic event and continued for 1 min following the melt. The melt baseline is projected in the conventional manner from the point of melt (or eutectic) onset to the melt conclusion. An exception to this baseline projection was required with some very small eutectic events where the subsequent melt curve dropped below the baseline projection: an alternate baseline projection was then started at the lowest point after the eutectic event.

The large volume of digitized data and multitude of computations are best handled by computer. Until recent interfacing of the DSC with a data acquisition and processing system, data were entered manually. A typical computer input/output is shown in Fig. 2. For the sake of brevity and clarity some printed computer/operator dialogue has been omitted, such as the manual input of data and corrections. The data, displayed in Fig. 2, are presented in an orderly array as an aid to proof-reading the manual entries for possible corrections. Since a data point must represent the accumulated melt during the integration period, as shown by the shaded area in Fig. 3A, a distinction between "integrated" and "digitized" data is required. An "integrated" data point is the accumulation of the changing signal within the time (integration) period and therefore the electrical equivalent of the accumulated melt during that period. However, the curve height measurement only at the conclusion of the time period, and simplified for this discussion as "digitized", must be averaged with the previous measurement to give an equivalent "integrated" data point. This is necessary before proceeding with the derivations that follow.

For changing electrical data to calories, the melt area of a reference standard, such as indium, is measured for the calibration factor. This factor, combined with sample weight, molecular weight and signal range, provides the final "conversion factor" to convert the melt data to cal mole^{-1}. The last

```
DSCPURB
CMPD NAME OR CODE ? ?ACETANILIDE  CHN REF STD
 LOT # ? GMG 2-10-58      2ND MELT
 Date of Scan ?5/10/77
 Molecular Wt ?135.16
Sample Wt ?4.50634 ( mg )
Calibration Factor ?.00002494 ( mcal/Mv-sec )
 Heat Rate ?10 ( deg/min )
 Range ?10 ( Mv-full scale )
Seconds, I Integrated (1), or Digitized (D) ?2,I
 Initial Temp ?384
```

	0	1	2	3	4	5	6	7	8	9
0		2951	2970	3001	3030	3053	3081	3119	3160	3251
10	3359	3646	4783	9009	16740	25915	34026	42304	48216	52367
20	55063	56335	56463	56931	56641	56853	55993	51273	39036	23096
30	12389	7221	5203	4446	4192	4094	4070			

```
Temp Immediately Preceeding Melt Onset =  385.667
BASELINES: Initial=  3081          Final=  4070
Base Change / Step =  32.9667          Temp Change / Step =  .333333
Conversion Factor =  7.53942E-03     Cal/Mol-Mv
TOTAL Accum Melt =     5206.457 Cal/Mol

Acceleration Peaks are found at STEP   18      7
Maximum Acceleration is at STEP  7
```

Step	Av Melt	1st Deriv	2nd Deriv	3rd Deriv	Accum Melt
.5		.038		.004	
1	.038		.023		.038
.5		.061		.204	
2	.099		.226		.136
.5		.287		.204	
3	.385		.430		.522
.5		.716		.769	
4	1.102		1.199		1.623
.5		1.915		5.210	
5	3.017		6.409		4.641
.5		8.324		16.881	
e- 6	11.341		23.289		15.981 d
.5		31.613		3.136 k	
e- s- 7	42.954 e h		26.426		58.935 H
.5		58.039 v		-15.539 u	
8	100.993 e		10.887		159.928
.5		68.926		-12.877	
9	169.918		-1.990		329.846
.5		66.935		-8.437	
10	236.853		-10.427		566.699
.5		56.508		-2.134	
11	293.362		-12.561		860.061
.5		43.948		-.339	
12	337.309		-12.900		1197.370
.5		31.048		1.930	
13	368.357		-10.970		1565.727

```
Evaluate Other Peaks, YES or NO N
Calculate RESULTS based on which Accel. Peak 7
          Interpolation Factor =  .167945
    for which 3rd Deriv = ZERO

SLOPE =  2.41589E-03
  1/F =  116.548
TEMP KO =  368.171
Heat of Fusion   5206 Cal/Mol

          IMPURITY =  4.20121E-03     MOL %
```

Fig. 2. Impurity computation for acetanilide (see chart trace in Fig. 3A).

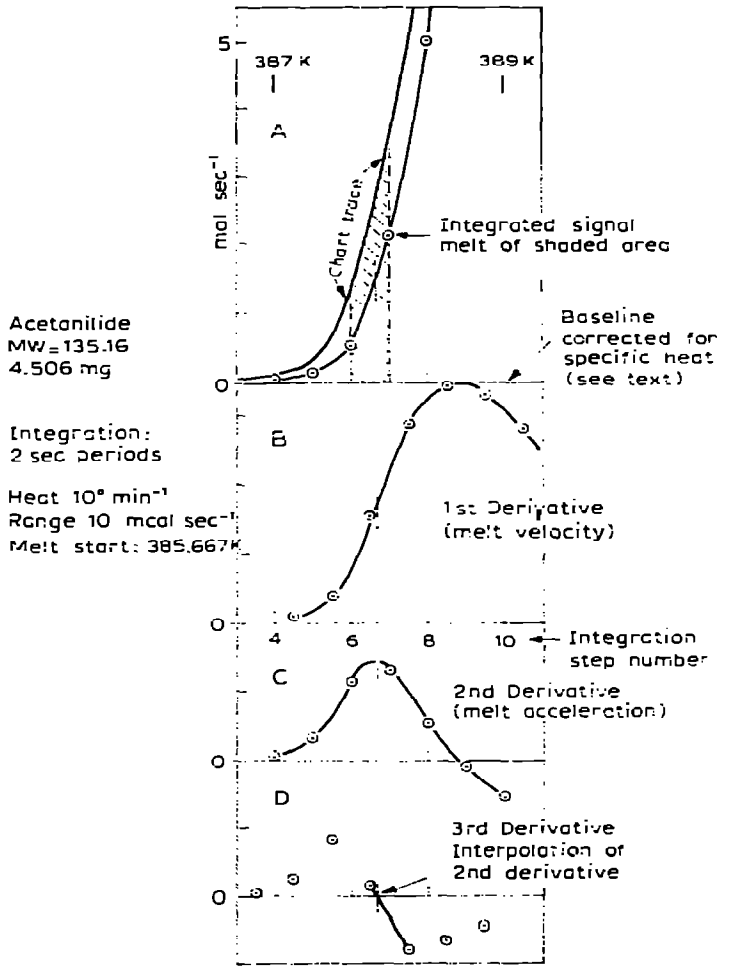

Fig. 3. DSC chart trace and integrated signal with derivatives (computed in Fig. 2).

point of the initial baseline is selected by the computer where the following projected melt baseline slope is greater than the difference between preceding data points. In Fig. 2, the last of the initial baseline is data point 6 with the first melt step being data point 7. Along with the integrated or "average melt" at each step (displayed as cal mole^{-1}), the "accumulated melt" is summed in the extreme right column. The "total accumulated melt" shown above the columns of derivatives is also more appropriately identified at the bottom as "heat of fusion" and is the value, H, in the "Definition of Terms" below.

In Figs. 2—4, only that portion of an acetanilide melt which surrounds the moment of maximum acceleration is illustrated for simplicity. In Fig. 2, the subtractions between melt steps for the derivatives, and the accumulated melt summations are self-evident. However, the subsequent computations are illustrated below.

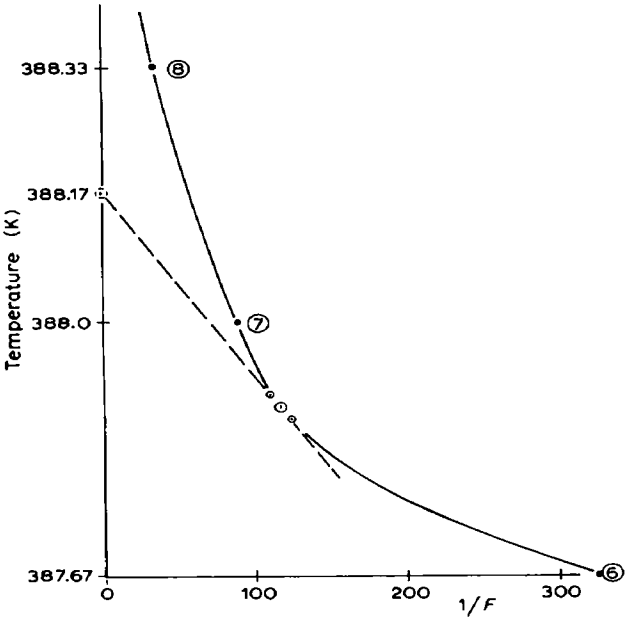

Fig. 4. Temperature vs. $1/F$ for acetanilide (as computed in Fig. 2). •, Integration step number in circles; ⊕, theoretical melting point; ⊙, point of maximum acceleration; ⊙, melting rate (tangential slope) about point of maximum acceleration. — — —, Projection of melting rate to $1/F = 0$.

Definition of terms

The small-lettered terms below are also circled in Fig. 2 beside the appropriate data associated with the step of maximum acceleration. Computed results are identified by capital letters.

a 3rd derivative preceding maximum 2nd derivative (at step 7 in Fig. 2)
b 3rd derivative following maximum 2nd derivative
I interpolation factor for which 3rd derivative = 0 (see Fig. 3D)
P computed point of maximum acceleration (see Fig. 3C)
c average melt at step following point of maximum acceleration, *P*
d accumulated melt at step preceding point of maximum acceleration, *P*
e step No. preceding point of maximum acceleration, *P*
Note: When $I > 0.5$, the maximum acceleration, *P* is in the next step, and the positions *c*, *d*, and *e* are also located in the next step at *c'*, *d'*, and *e'* for the appropriate data.
h average melt at step *e'*
v melt velocity following step *e'*
g last positive 3rd derivative step midway between *e* and *e'* before maximum acceleration
A accumulated melt at point of maximum acceleration, *P*
H total accumulated melt (molar heat of fusion)
M melt rate at point of maximum acceleration, *P*

$1/F$ reciprocal of fraction melted at point of maximum acceleration, P (see Fig. 4)
S tangential slope at point of maximum acceleration, P (see Fig. 4)
T_0 theoretical melt of pure substance (Fig. 4) where S intercepts the temperature scale at $1/F = 0$

Calculations (refer to Figs. 2 and 3)

For a second approximation of the maximum acceleration (2nd derivative) point, the interpolation factor, I, at which the 3rd derivative equals 0 is estimated. By using a line between the 3rd derivative points a and b, as shown in Fig. 3D, interpolation is the amount of a above zero in proportion to total line a—b.

$$I = a/(a - b) \tag{2}$$

$$= 3.136/[3.136 - (-15.539)] = 0.1679$$

The point at maximum acceleration becomes

$$P = g + I \tag{3}$$

$$= 6.5 + 0.1679 = 6.6679$$

The melt that has occurred during the fractional step between e and P is computed from the average melt at c and added with the previous accumulated melt at d to establish the accumulated melt, A, at point P

$$A = c(P - e) + d \tag{4}$$

$$= 42.954\ (6.6679 - 6) + 15.981 = 44.672\ \text{cal mole}^{-1}$$

The reciprocal of the fraction melted, $1/F$, at maximum acceleration becomes

$$1/F = H/A \tag{5}$$

$$= 5206/44.672 = 116.54$$

Melting rate at maximum acceleration determines the tangential slope at $1/F$, shown in Fig. 4. This rate is the sum of the computed velocity at I and the average melt immediately preceding it.

$$M = vI + h \tag{6}$$

$$= 58.039\ (0.1679) + 42.954 = 52.701\ \text{cal/mole-step}$$

The accumulated melt immediately before and after the point $1/F$ in eqn. (5) provides two additional points through which a straight line can be established as the tangential slope to the curve. Errors from the unsymmetrical curvature shown in Fig. 4, and the constantly changing melting rate are minimized by selecting very small temperature increments (T_1, T_2) of only $0.05 \times \Delta T$/step (heating rate) on either side of the point $1/F$. At these incremented temperature positions, accumulated melts A_1 and A_2 differ from A by the same increment (0.05) in the melting rate

$$A_1 = A + 0.05 \times M \tag{7}$$

$$A_2 = A - 0.05 \times M \tag{8}$$

Their corresponding reciprocal-of-the-melt-fraction become

$$1/F1 = H/A_1 \tag{9}$$

$$1/F2 = H/A_2 \tag{10}$$

The total temperature incremented between A_1 and A_2 is

$$T_1 - T_2 = 0.1 \times \Delta T/\text{step (heating rate)} \tag{11}$$

The tangential slope through the two points becomes

$$S = (T_2 - T_1)/(1/F2 - 1/F1) \tag{12}$$

Substituting eqns. (7), (8) and (11) into (12)

$$S = (0.1\ \Delta T/\text{step})/[H/(A + 0.05\ M) - H/(A - 0.05\ M)] \tag{13}$$

$$= (0.1 \times 0.333)/[5206/(44.672 + 0.05 \times 52.7) -$$

$$5206/(44.672 - 0.05 \times 52.7)]$$

$$= -0.002416$$

Projection of this tangential slope, S, to $1/F = 0$ gives the theoretical melt temperature of pure substance, T_0.

$$T_0 = \text{melt onset (at step)} - S(1/F) + P(\Delta T/\text{step}) \tag{14}$$

$$= 385.667 - (-0.0024)\ 116.54 + 6.6679 \times 0.333$$

$$= 388.17\ \text{K}$$

Finally, by rearranging the slope in the van't Hoff expression, eqn. (1), where

$$S = \frac{XRT_0^2}{H} \tag{15}$$

the mole fraction, X, is converted to percent.

$$\text{mole \% impurities} = 100X = 100(SH)/RT_0^2 \tag{16}$$

$$= \frac{100 \times 0.002416 \times 5206}{1.987 \times 388.17 \times 388.17}$$

$$\text{impurities} = 0.0042\ \text{mole \%}$$

DISCUSSION

Remarkably broad ranged impurity levels from $<10^{-4}$ to 50 mole % have been measured. Phenacetin spiked with benzamide at levels ranging from 1 to 51 mole % gave results (shown in Table 1) with an overall variability of ±5% RSD. At 50 mole % a variability of ±2 mole % was obtained.

Mixtures which do not have the wide temperature gap between the eutectic and final melt shown in Fig. 1 cannot be measured above an impurity

level where resolution of the final melt phenomenon is masked by the preceding eutectic event. This masking will be more acute where the impurity level approaches the eutectic composition. At such levels, the question arises as to which component does the final melt represent. A phase diagram might be required. Such an experimental diagram of phenacetin/benzamide by Marti [4] showed its eutectic phase to contain about 35—40% phenacetin.

Integration period and signal noise have a significant effect on accuracy. Results from longer integrations with the same raw data are shown in Tables 1 and 2. They were computed after summing the "average melts", shown in

TABLE 1

DSC purity analysis of phenacetin spiked with benzamide: effects of heat, integration rate, and heat transfer enhancement with silicone grease

Benzamide (mole%)	Mole% impurity found		
	5°C min^{-1}	10°C min^{-1}	10°C min^{-1} + silicone on pan base
0	0.58 (2) 0.61 (6) 0.44 (12)	0.22 (1) 0.23 (2) 0.29 (4)	
1.48		1.88 (6) 1.85 (12) 1.87 (18)	1.72 (6) 1.23 (12) 0.86 (18)
3.03		3.17 (6) 2.87 (12) 2.33 (18)	3.02 (6) 2.95 (12)
7.94		8.50 (6) 8.51 (12) 8.41 (18)	7.95 (6) 7.34 (12)
12.83		12.71 (6) 12.53 (12) 12.49 (18)	12.00 (6) 11.66 (12)
17.87		17.38 (6) 17.07 (12) 16.35 (18)	16.93 (6) 16.57 (12)
21.18	19.70 (4) 19.67 (8) 19.68 (12)	21.46 (2) 21.44 (4) 21.08 (6)	
30.78		30.61 (6) 30.62 (12) 30.33 (18)	30.21 (6) 30.26 (12)
33.86	32.80 (4) 32.73 (8) 32.68 (12)	33.74 (6) 33.50 (12)	
51.05	48.16 (2) 48.01 (4)	52.07 (1) 52.10 (2)	

Parentheses denote integration period in seconds — results for larger integration intervals computed from same data as the smallest interval shown in each group.

TABLE 2

DSC purity analysis of zinc *: effects of heating and integration periods

Integration ** period (sec)	Mole% impurities Heating rate (°C min^{-1})		
	2.5	5	10
2			0.0014
4		0.0017	0.0028
6	0.0015		0.0029
8		0.0027	
12	0.0032	0.0026	
18	0.0063		

* Perkin-Elmer Corp. (no stated purity) DSC melt reference standard.
** Results of larger integrations under each heating rate are computed from the same data as the results at the smallest integrations shown.

Fig. 2, in groups of 2, 3, or 4 to give the equivalent multiple of the lowest period noted. A 1-sec integration would be most practical for fast melting materials with <0.01% impurities, such as the zinc in Table 2, since resolution rapidly diminishes using the longer periods. Yet the burden of manually entering more than 50 data points makes the longer integration periods more practical where adequate resolution can still be retained. A decided advantage with longer integrations is the increase of signal to noise. This proved more effective than electronic noise filtering through the typical resistor/capacitor network of the instrument. However, longer integrations of slower melts may still cause an unacceptable loss of resolution in the final melt where preceding eutectic events are close.

Variable sample and pan contact have created sporadic curve changes during the melt to present a noise problem. The 2nd derivative tabulations (shown in Fig. 2) may require a careful selection of the most consistent acceleration data over spurious, and sometimes larger, acceleration peaks. However, the method appears independent of consistent thermal resistance. Glass wool placed under the sample pan drastically changed the melt curve shape and offset the temperature scale but did not alter the indium results shown in Table 3. Enhancing the pan contact with the heater by using a small amount of silicone grease on the pan base also reduces vibration problems without serious bias of the results (Table 1). Yet two undesirable features occur with the use of grease: it cannot be heated beyond its heat-stable range for there must be no thermal transitions from it, and its complete removal from the heater chamber is essential afterwards.

The results are independent of heating rate within practical limitations. The heating rate must be sufficiently fast to give a large enough rate of acceleration above the signal noise, yet it must not be so fast as to lose the needed resolution during the melt. The independence from integration period has similar practical limitations but in a reverse sense. The integration period must be sufficiently long to average noise effects, but short enough to retain

TABLE 3

DSC purity analysis of indium *: effects of weight, heating rate **, and thermal resistance

Heating rate (°C min^{-1})	× 10^{-5} mole% impurities Indium weight (mg)			
	0.7		7	75
0.31	17		1.4	1.2
0.62			2.1	
1.25	12	1.9 ***	2.8	0.3
2.5			4.2	
5	24	3.2 ***	5.9	1.7
10			12	2.3

* Perkin-Elmer, DSC reference standard, purity 99.9999% [1].
** With 1 sec integration.
*** Glass wool under sample pan to drastically decrease thermal conductivity.

the desired resolution. As a general rule to follow, faster heating rates require shorter integration periods. Sample weight, although not critical, can be increased to enhance the signal to noise and resolution as needed. The effects of a 100-fold difference in indium sample size coupled with a 10-fold difference in heating rate are shown in Table 3; integration was held at 1-sec intervals.

These results may be below the lowest detectable level for any practical use. Maximum acceleration at this high purity occurs within several seconds of melt start for 7 mg of indium, and within 6—12 sec for 75 mg. Materials having documented impurities in this range of 10^{-4}—10^{-5} mole % are needed to establish the lowest detectable level. Indium was used as the calorimetric reference for other materials. No attempt was made to convert its melt area into calorimetric equivalents with another reference material. Instead, its melting point (429.78 K) and heat of fusion (779.6 cal mole^{-1}) were substituted directly into eqn. (15).

Along with the sources of variability mentioned above is the addition of experimental errors in measuring the heat of fusion, H, and the extrapolated melting temperature, T_0. "Pure" phenacetin in Table 1, having a very narrow melting range with no eutectic events, gave a heat of fusion of 8200 ± 100 cal mole^{-1}, yet the spiked samples with a eutectic event and broad melting range gave a heat of fusion of 7800 ± 200 cal mole^{-1} independent of the impurity level. The computed T_0 ranged from 405 to 412 K, varying as much from different heating rates as from other factors. The unspiked phenacetin shows some impurities. A regression analysis of the phenacetin results, those having the shortest integration period, gives a good correlation coefficient of 0.9988. But a slope of 0.975, being less than unity, would suggest a consistent bias; due perhaps to the heat of fusion measurements. The other regression statistics are: standard error of the slope, 0.011; intercept, 0.18 mole %; standard error of the intercept, 0.27 mole%; standard error of estimate, 3.42;

TABLE 4

DSC purity analysis of various compounds

Compound	Impurity (mole%)	Source
Acetanilide	0.0052, 0.0042, 0.0035	1
p-Anisic acid	0.37, 0.29	1
Anthracene	0.021, 0.014	2
3,4-Dichloroaniline	0.11, 0.11	
Dimethyl fumarate	1.90, 1.92	
Diphenyl phosphinic acid	0.08, 0.11	3
Phenacetin	0.06, 0.09	
S-Benzylthiuronium chloride	0.38, 0.40	2 (a)
Toluic acid	0.040, 0.035, 0.033	1
2,4,5-Trichlorophenol	1.58, 1.60	5
Zinc	0.0013, 0.0014, 0.0017	4
Test substance	1.97, 1.97	6

Sources:

1 Aldrich, zone refined.
2 British Drug House, microanal standard, (a) labeled <0.5 impurities.
3 Ultrex, zone refined, labeled assay 99.84, 99.90 (titration).
4 Perkin-Elmer, DSC reference standard.
5 Dow Chemical.
6 Digitized melt data provided by Perkin-Elmer after their evaluation by their original dynamic procedure gave results of 1.73, 1.88 mole%.

standard deviation about regression line (residuals), 0.807.

A more practical approach for eqn. (15) would be to use known values for H and T_0 that have been either published in the literature or established with essentially pure substances. This leads to a possible simplification of the entire purity procedure. First, no sample weights, molecular weights, conversion factors, signal ranges, nor temperature onsets would be needed. The operator would use an unweighed sample and introduce into the computations the known values for H and T_0, the programmed heating rate, and the integration period. The melt data manipulations would be reduced considerably since no conversions to calorimetric equivalents are needed. The partial melt and melting rate at maximum melt acceleration are only relative to the total area irrespective of other factors. Such a simplification would make the procedure ideal for fast routine, quality control applications.

SUMMARY

The dynamic melting process is affected by numerous variables: specific heat, thermal resistance, heating rate, and sample size are the more obvious ones. By computing the 2nd derivative of the melt data, the variables' conflicting effects are minimized, if not totally removed, at the 2nd derivative peak (maximum acceleration of the melting rate). The melting rate at this peak provides the rate change of $1/F$, or impurity slope, in the van't Hoff plot. This permits extremely broad ranged impurity measurements not

previously possible; the upper limit of detection being dependent on adequate resolution of the final melt curve following preliminary eutectic events. Impurities from $<10^{-4}$ to 51 mole % have been measured with a RSD of 5%.

Data manipulation is best handled by computer. The total melt area being measured includes eutectic areas. Signal to noise is enhanced with a combination of faster heating rates (5—20°C min^{-1}), larger samples (10—20 mg), and longer integrations (2—6 sec). However, adequate resolution for very pure materials (<0.01 mole % impurities) necessitate slower heating rates (2.5—5°C min^{-1}) and short integrations (1 sec).

The mathematical model has been applied only to data from the Perkin-Elmer DSC-2 instrument. It is not known if this principle is applicable to other thermal analyzers which do not use similar active heater feedback circuitry to control the melt process.

This new purity method does not extend beyond the material limitations that have been previously detailed [3]. Briefly, the impurities must be insoluble in the solid phase but soluble in the melt; there must be no decomposition or chemical rearrangements; and, for multiple crystal forms, the most stable crystal form must be analyzed. Remelts of a sample are recommended for computations, for the initial melt frequently is not the most stable crystal form.

Mathematically derived curve smoothing procedures seem most appropriate to cope with the variety of noise problems mentioned in the discussion. This approach coupled with a fast (1 sec) integration rate is being pursued to enhance the resolution and, thus, the precision and accuracy with heating rates up to 40°C min^{-1}.

REFERENCES

1 Therm. Anal. Newsl., No. 5, Perkin-Elmer Corp., Norwalk, CT, 1965.
2 Therm. Anal. Newsl., No. 6, Perkin-Elmer Corp., Norwalk, CT, 1966.
3 C. Plato and A. Glasgow, Anal. Chem., 41 (1969) 330.
4 E. Marti, Thermochim. Acta, 5 (1973) 173.
5 United States Pharmacopeia, XIX, Thermal Analysis, (1975) 714.
6 H. Staub and W. Perron, Anal. Chem., 46 (1974) 128.
7 A.P. Gray, Thermal Analysis Application Study, No. 3, Perkin-Elmer Corp., Norwalk, CT, 1972.
8 A.P. Gray and R.L. Fyans, Thermal Analysis Application Study, No. 10, Perkin-Elmer Corp., Norwalk, CT, 1973.
9 J. Zynger, Anal. Chem., 47 (1975) 1380.